

## Quaternary base-level drops and trigger mechanisms in a closed basin: Geomorphic and sedimentological studies of the Gastre Basin, Argentina



Andrés Bilmes<sup>a,\*</sup>, Gonzalo D. Veiga<sup>b</sup>, Daniel Ariztegui<sup>c</sup>, Sébastien Castellort<sup>c</sup>,  
Leandro D'Elia<sup>b</sup>, Juan R. Franzese<sup>b</sup>

<sup>a</sup> Instituto Patagónico de Geología y Paleontología – (CENPAT-CONICET), Boulevard Almirante Brown 2915, ZC: U9120ACD Puerto Madryn, Chubut, Argentina

<sup>b</sup> Centro de Investigaciones Geológicas (CIG), Universidad Nacional de La Plata - CONICET, La Plata, Argentina, Calle Diagonal 113 N8 275, B1904DPK La Plata, Argentina

<sup>c</sup> Section des Sciences de la Terre et de l'Environnement, Rue des Maraichers 13, 1205 Genève, Switzerland

### ARTICLE INFO

#### Article history:

Received 29 July 2016

Received in revised form 7 January 2017

Accepted 9 January 2017

Available online 24 January 2017

#### Keywords:

Lake shorelines

Climate change

Tectonic activity

Sediment routing system

### ABSTRACT

Evaluating the role of tectonics and climate as possible triggering mechanisms of landscape reconfigurations is essential for paleoenvironmental and paleoclimatic reconstructions. In this study an exceptional receptive closed Quaternary system of Patagonia (the Gastre Basin) is described, and examined in order to analyze factors triggering base-level drops. Based on a geomorphological approach, which includes new tectonic geomorphology investigations combined with sedimentological and stratigraphic analysis, three large-scale geomorphological systems were identified, described and linked to two major lake-level highstands preserved in the basin. The results indicate magnitudes of base-level drops that are several orders of magnitude greater than present-day water-level fluctuations, suggesting a triggering mechanism not observed in recent times. Direct observations indicating the occurrence of Quaternary faults were not recorded in the region. In addition, morphometric analyses that included mountain front sinuosity, valley width–height ratio, and fan apex position dismiss tectonic fault activity in the Gastre Basin during the middle Pleistocene–Holocene. Therefore, we suggest here that upper Pleistocene climate changes may have been the main triggering mechanism of base-level falls in the Gastre Basin as it is observed in other closed basins of central Patagonia (i.e., Carri Laufquen Basin).

© 2017 Elsevier B.V. All rights reserved.

### 1. Introduction

Understanding Earth's history and predicting the response of surface systems to global changes are at the heart of current research in Earth Science. In particular, the documentation of tectonic and climatic signals in source-areas is crucial to understanding their propagation within entire sediment routing systems and their eventual deposition in sedimentary basins (Castellort and Van Den Driessche, 2003; Allen, 2008; Simpson and Castellort, 2012; Whittaker, 2012).

Internally drained basins, also known as endorheic basins, are very sensitive to external factors such as climate change and tectonic activity because these factors have a direct impact on base-level changes and their geomorphic and sedimentary response within the basin.

The sensitiveness to tectonics and climate has made endorheic basins ideal laboratories for studying the history and role of tectonic and climate changes preserved in the Earth's geological record over ancient timescales (e.g., Carroll and Bohacs, 1999; Pochat et al., 2005) but also during the Quaternary (García-Castellanos, 2006; Ariztegui et al.,

2008; Mon and Gutiérrez, 2009; Howarth et al., 2012; Whittaker, 2012; Dorsaz et al., 2013). However, even in endorheic basins, distinguishing between tectonic and climate signals is not always an easy task. A same base level marker (e.g., ancient lake shorelines of a lake highstand) could be related either to climate variations (e.g., change from a wet to dry period; Gilli et al., 2005; Wünnemann et al., 2015) or to tectonic activity (e.g., drainage reorganization in response to tectonic uplift; Mon and Gutiérrez, 2009). Only a detailed base-level change documentation, combined with a paleoclimatic/tectonic understanding of the local systems, will provide the integrated overview necessary to either validate or reject the different possible scenarios.

The Patagonian Broken Foreland exhibits several closed lows that are filled with Neogene–Quaternary clastic and volcanic deposits (Fig. 1). At the latitude of the study area, these endorheic basins were unaffected by Andean glaciers during the last glaciation (Rabassa and Clapperton, 1990). The origin of these lows is related to active mountain fault block reconfiguration during the middle Miocene Andean orogeny. Inside these basins, major Quaternary base-level drops, indicated by fluvial incisions and terraces, or lake-level fluctuations, have been described since the pioneering works of Volkheimer (1965, 1973) and Proserpio (1978). However, the origin of these Quaternary base-level drops remains controversial even within individual topographic lows

\* Corresponding author.

E-mail address: [abilmes@cenpat-conicet.gob.ar](mailto:abilmes@cenpat-conicet.gob.ar) (A. Bilmes).

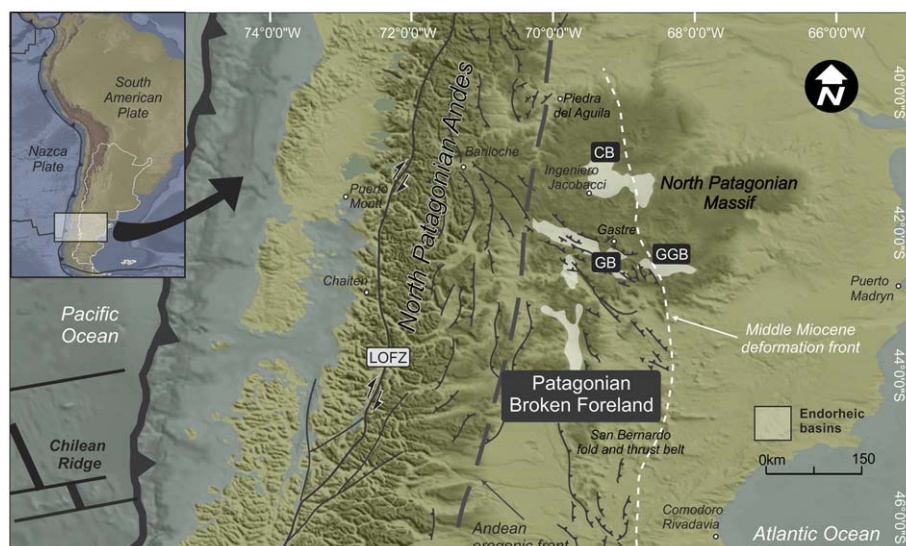


**Fig. 1.** The Gastre Basin as part of the Patagonian Broken Foreland. Simplified map of the North Patagonian Andes and the adjacent foreland where the Gastre Basin is located, showing main structures and distribution of Neogene to Quaternary endorheic basins (white areas). Base hillshade map constructed from an SRTM30 PLUS data set at 30 arc-second resolution. Global bathymetry data and SRTM elevation data at 3 arc-second resolution. GB: Gastre Basin; CB: Carri Laufquen Basin; GGB: Gan Gan Basin. LOFZ: Liquiñe-Ofqui fault zone.

(e.g., Gastre Basin or Carri Laufquen Basin) where evidence suggests neotectonic activity (e.g. fractures associated to a Quaternary volcanic field or basin asymmetry; Volkheimer, 1965, 1972; Regairaz and Suivres, 1984; Massaferrro et al., 2006) and Quaternary climate changes (Galloway et al., 1988; Bradbury et al., 2001; Ariztegui et al., 2008; Cartwright et al., 2011). This paper examines several base-level drops recorded in the Patagonian Broken Foreland within the Gastre Basin in a variety of geomorphic and sedimentary archives and explores their link with Quaternary climate change and neotectonic activity in the area. The main goals of this study are to reconstruct and analyse the behaviour of the Gastre Basin during the Quaternary and to establish the relative role of climate and tectonics in the Quaternary evolution of this closed basin. Understanding the origin of the Quaternary base-level drops is critical in any attempt to elucidate neotectonic activity in the Patagonian Broken Foreland. In addition, as many Quaternary base levels of this region were used to support global climate change reconstructions (e.g., Galloway et al., 1988; Bradbury et al., 2001; Cartwright et al., 2011), this work will provide helpful data for the Quaternary paleoclimate reconstruction of South America.

## 2. Geological and environmental setting: the Gastre Basin as part of the Patagonian Broken Foreland

The present landscape of the Patagonian Broken Foreland is characterized by several endorheic depressions filled with Quaternary deposits that are surrounded and separated by mountain blocks with elevations of up to 1900 m asl (e.g., Gastre Basin, Carri Laufquen Basin, Gan Gan Basin; Fig. 1). The spatial configuration of this intraplate setting is linked to the tectonic history of the region, defined by regional pre-Neogene, NW- and NNE-trending lineaments (Coira et al., 1975; Figari et al., 1996; Allard et al., 2011; Folguera and Ramos, 2011), that were reactivated or inverted during the main stage of Andean contraction in the middle Miocene (Bilmes et al., 2013). Since the late Miocene, the Patagonian Foreland is subjected to a regional uplift at a rate of ~0.14 m/ka (Guillaume et al., 2009; Pedoja et al., 2011; Folguera et al., 2015).

The Gastre Basin (Dalla Salda and Franzese, 1987) is one of the largest internally drained basins of the Patagonian Broken Foreland (Fig. 2). It has a NW-SE main trend, oblique to the Andean chain, and extends over an area of 4200 km<sup>2</sup>. It was originated in the middle Miocene (16.1–14.86 Ma) by reverse faulting and inversion of pre existing

normal faults (Bilmes et al., 2013). Paleozoic–Lower Miocene igneous and sedimentary rocks constitute the basin basement. The heights of the NE-bounding mountains (~1800 m asl) are higher than the ones in the SW (~1200 m). The basin floor (at ~840 m asl) is broken by internal basement highs (e.g., Sierra del Medio, Cerro Bota, and Loma Alta hills; Fig. 2) that delineate four depressed areas, each of which has a playa lake fed by NE–E ephemeral streams (e.g., Calcatapul River system or the Gastre River system; Fig. 2).

The basin infill comprises a middle Miocene to Quaternary succession that includes continental deposits and volcanic rocks (Bilmes et al., 2014). The Neogene deposits—La Pava Formation (Nullo, 1978), Collón Cura Formation (Yrigoyen, 1969), and Río Negro Formation (Volkheimer, 1973)—are mainly in the subsurface and crop out essentially in areas where important fluvial incision occurred (e.g., east bank of the Río Chico; Fig. 3). In contrast, Quaternary deposits are distributed all over the Gastre Basin where they crop out in the piedmont slope and in the basin floor (Fig. 3). The Quaternary sedimentary record is composed of a 10 to 150-m-thick succession that includes sedimentary deposits of the Choiquepal Formation (Volkheimer, 1964), volcanic basaltic rocks of the Moreniyeu and Crater formations (Ravazzoli and Sesana, 1977; Proserpio, 1978), and alluvial and fluvial deposits that have not yet been attributed to a formal lithostratigraphic unit (Ravazzoli and Sesana, 1977; Nullo, 1978; Proserpio, 1978; Volkheimer and Lage, 1981; Regairaz and Suivres, 1984; Bilmes, 2012).

Modern climate around the Gastre Basin is arid with a mean annual temperature of 18 °C and a mean annual rainfall of 150 mm, dominated by winter rainfall patterns (CNEA, 1990). Terrain and river network geometry analyses suggest a certain degree of topographic and drainage asymmetry for the Gastre Basin (Regairaz and Suivres, 1984; Bilmes, 2012). Higher mountain fronts and larger drainage basin areas are located in the NE border, whereas lower mountain fronts and smaller drainage basin areas dominate the SW border (Fig. 2).

## 3. Methodology

This work includes an exhaustive tectonic geomorphology analysis of the region (Fig. 4), the construction of a geomorphological-sedimentological map of the Gastre Basin (Fig. 5), and paleohydrological reconstructions associated with the Quaternary units. These issues were performed by assessment and mapping using map and imagery laboratory data and detail field work.



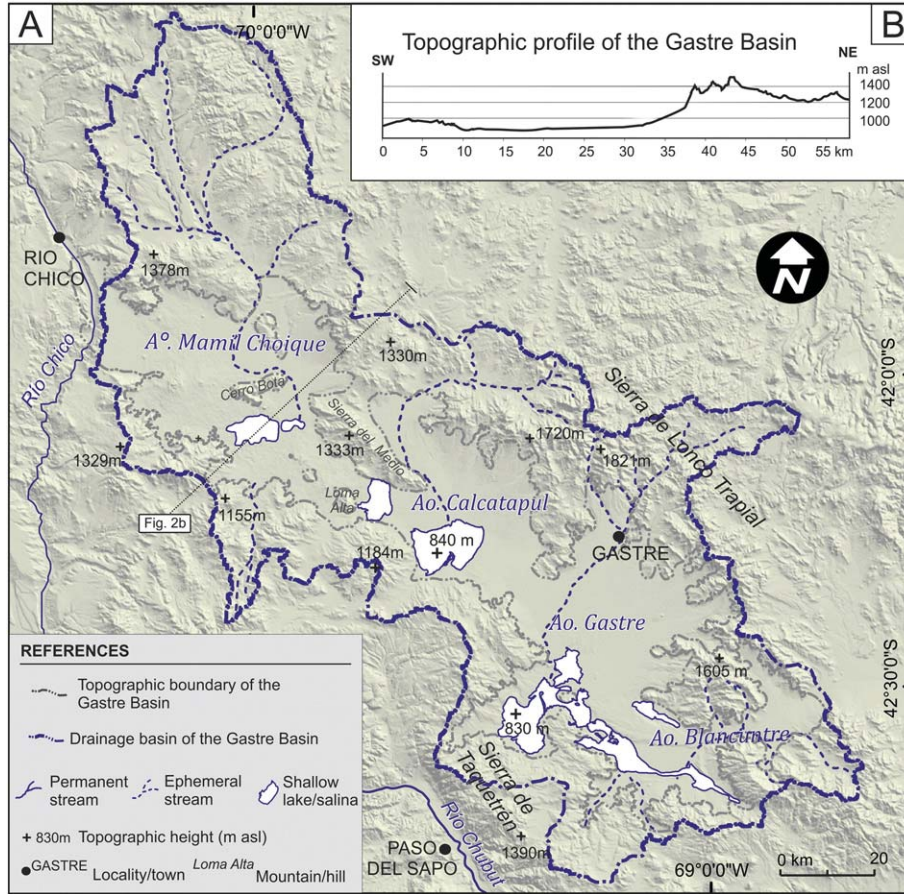


**Fig. 2.** (A) Hillshade map of the Gastre Basin showing major rivers, topographic heights and geographic locations referred to in the text. (B) Topographic profile across the Gastre Basin. Note the topographic and drainage basin asymmetry observed in both figures. Base hillshade map and topographic profile constructed from SRTM elevation data, 3 arc-second resolution (90 m).

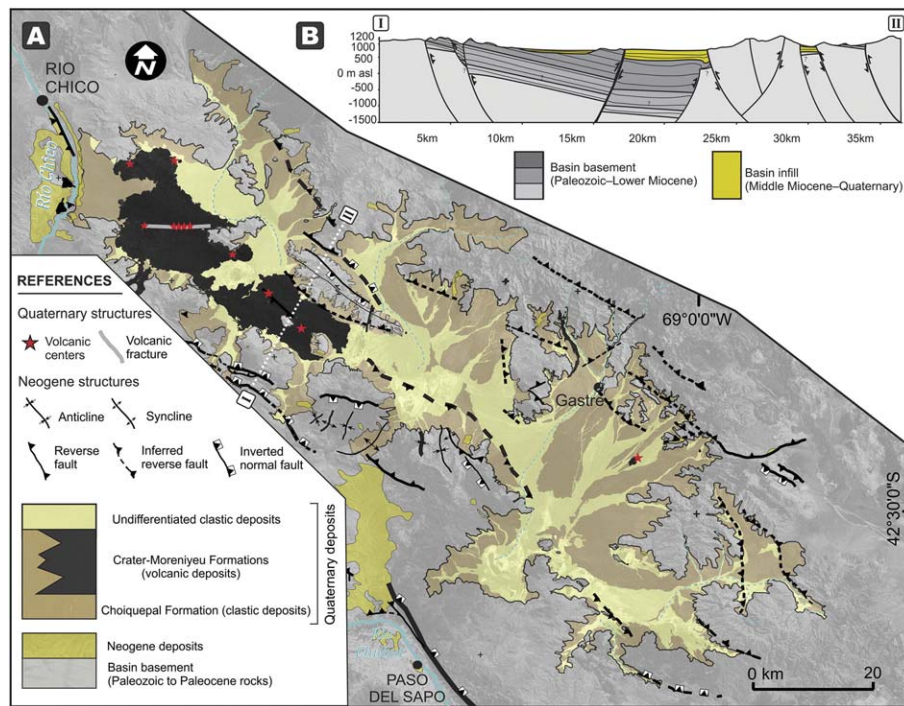


**Fig. 3.** (A) Geological map of the Gastre Basin with focus on the Neogene–Quaternary basin fill. Note fractures associated with volcanic vent alignment. (B) Geological cross section of the Gastre Basin. The trace of the cross section is indicated in (A).



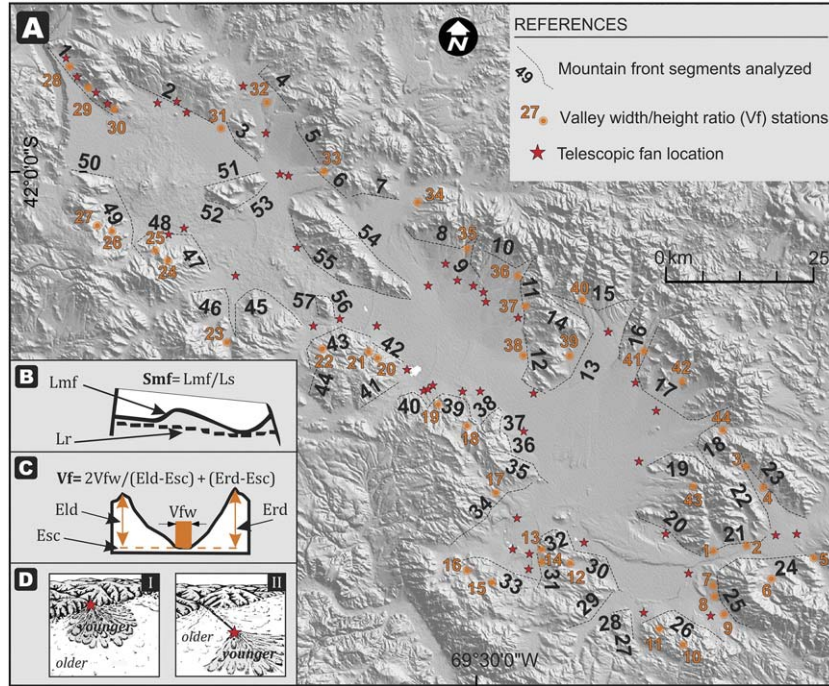


**Fig. 4.** Morphometric data set used in the tectonic geomorphology analysis of this study. (A) Location map. (B) Mountain front sinuosity index (*Smf*): mathematical derivation and measurement procedure. (C) The valley width/height ratio (*Vf*): mathematical derivation and measurement procedure. (D) Morphology of segmented fans and bajadas: (I) Inactive mountain front type, (II) active mountain fronts type, modified from (Bull, 1977). *Lmf*: length of mountain front along the mountain-piedmont junction; *Ls*: straight-line length of the front; *Vfw*: width of valley floor; *Eld* and *Erd*: respective elevations of the left and right valley divides; *Esc*: elevation of the valley floor.

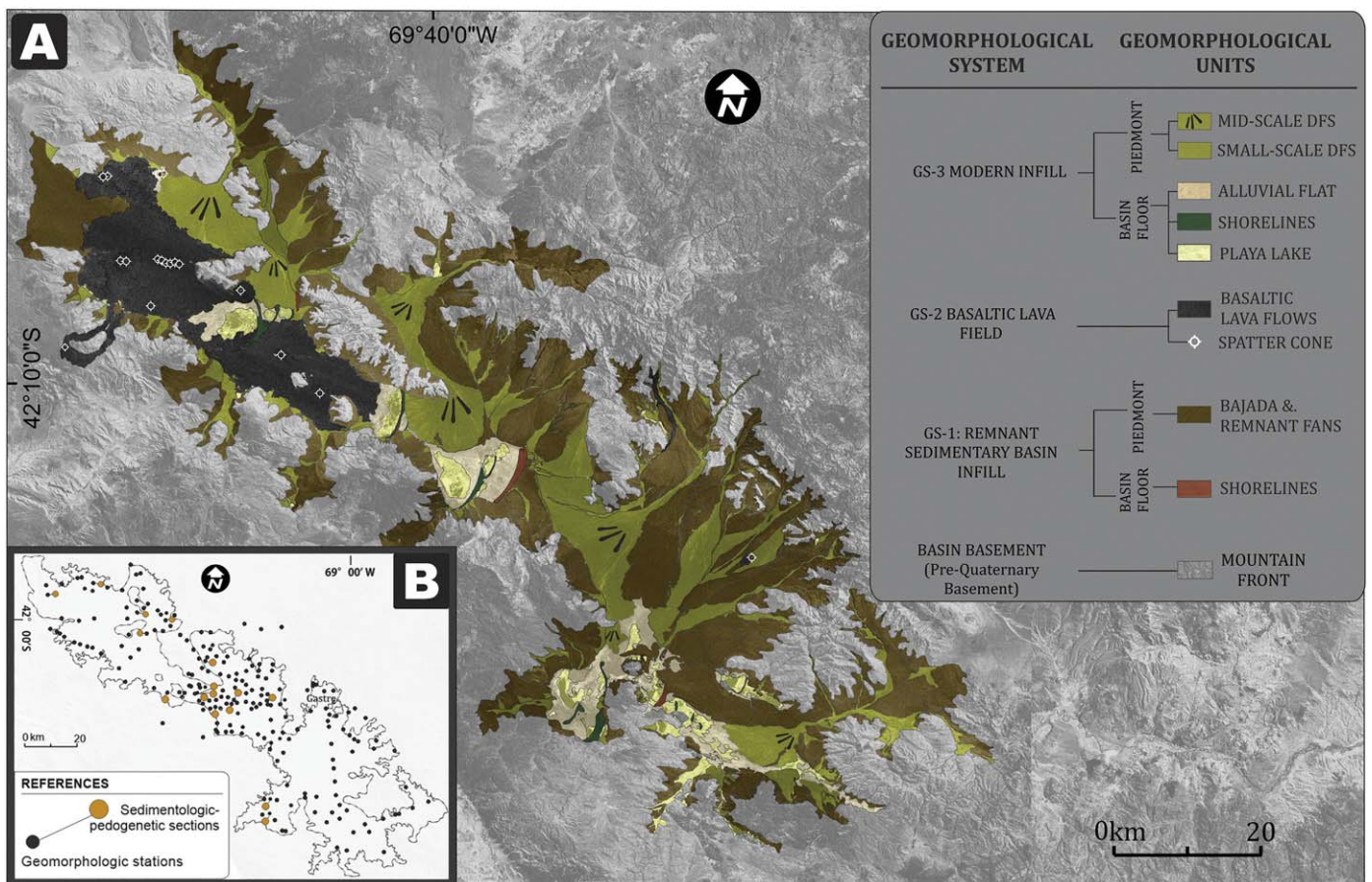


**Fig. 5.** Quaternary deposits of the Gastre Basin. (A) Geomorphological units and systems defined in this work. (B) Location map of geomorphologic and sedimentologic-pedogenetic sections.

### 3.1. Base mapping and geomorphological analysis

The ALOS-AVNIR images (spatial resolution of 10 m), ALOS PRISM images (spatial resolution of 2.5 m), and SRTM-3 DEM data (spatial resolution of 90 m) were used and analysed with ArcGIS© and SAGA GIS© softwares in order to construct a base map of the region. Field observations were performed at different scales including a total of 191 individual locations (see Fig. 5B). Observations on these stations focused on the relative degree of surface erosion of Quaternary units (i.e., presence gravels with desert varnish and ventifacts) and on documenting evidence of neotectonic fault scarps. To provide a hierarchical classification of the main landforms, an adaptation of Peterson's method (1981) was used. Morphology of the landforms were combined with genetic relationships and sedimentological data. Following this scheme, the Quaternary fill of the Gastre Basin was grouped into three major geomorphological systems that are composed of an arrangement of smaller elements defined as geomorphological units (Fig. 5).

### 3.2. Sedimentological analysis and paleohydrological reconstructions

In order to determine the main depositional characteristics of the Quaternary units, 16 sedimentologic-pedogenetic sections (Fig. 5B) were performed. These sections were concentrated on the description, sampling, and facies analysis of 100–180 cm deep pits and cores.

Paleohydraulic reconstructions of the basin were established using the geomorphological maps constructed in this work, combined with the sedimentological analysis, SRTM-3 DEM data, satellite images of the past 30 years (available from the USGS Center for Earth Resources Observation and Science; see <http://earthexplorer.usgs.gov>), and ArcGIS©toolbox. Elevation of the landforms was determined using the SRTM-3 DEM that has, in the study area, a relative height error of <5.5 m and an absolute geolocation error of <9 m (Rodríguez et al., 2006).

### 3.3. Tectonic geomorphology analysis

In order to analyse potential neotectonic activity in the region and in addition to field observations, different tectonic geomorphic indices were assessed using a base map data set, including (i) mountain front sinuosity index, (ii) valley width-height ratios, and (iii) alluvial/fluviol fan apex position (Fig. 4).

The *Mountain front sinuosity index* ( $S_{mf}$ ; Bull and McFadden, 1977) is defined as the ratio between the curvilinear length of the mountain piedmont front ( $L_{mf}$ ) and its straight-line length ( $L_s$ ; Fig. 4B). Range fronts associated with active tectonics are usually relatively straight with low  $S_{mf}$  values. Instead, slightly active or inactive mountain fronts have embayed range fronts with  $S_{mf}$  values > 1.8 (Bull and McFadden, 1977; Bull, 2007; El Hamdouni et al., 2008; Rockwell et al., 1984; Silva et al., 2003). In order to carry out the  $S_{mf}$  analysis of the study area, the surrounding mountain fronts of the Gastre Basin were subdivided into 57 discrete segments following the overall criteria proposed by Wells et al. (1988) (Fig. 4A).

The *Valley width/height ratio* ( $V_f$ ; Bull and McFadden, 1977) is defined as the ratio of the width of the valley floor to its average height (Fig. 4C). Where  $V_{fw}$  is the width of the valley floor, and  $E_{ld}$ ,  $E_{rd}$ , and  $E_{sc}$  are the elevations of the left and right valley divides and the elevation of the valley bottom, respectively. Low  $V_f$  values are typically associated to V-shaped valleys created by prolonged incision and uplift, generally indicative of active mountain fronts. Instead, high values of  $V_f$  are associated with U-shaped valleys generated in inactive mountain fronts by valley widening and ridge-crest lowering. Notably, the surrounding mountain fronts of the Gastre Basin have been unaffected by Andean glaciers during the last glaciation (Rabassa and Clapperton, 1990) ruling out U-shaped glacial valleys. In order to carry out a  $V_f$  analysis, 44 sites were measured and analysed (Fig. 4A).

Alluvial/fluviol fan apex position in the piedmont zone are complementary markers that can be used to evaluate tectonic stability of a mountain front (Bull and McFadden, 1977; Burbank and Anderson, 2005; Bull, 2007). Active mountain fronts typically have sediment deposition close to the front in response to high accommodation created along the mountain fault blocks at the proximity of the topographic break, topographic loading, and fault-induced subsidence (Simpson, 2014). In these cases, a pattern of fan-head positions close to the mountain front-piedmont junction is expected because high rates of subsidence induce headward back fill of feeder valleys (Fig. 4DI). In contrast, inactive mountain fronts have streams that bypass the mountain front in response to low accommodation near it and typically incise fan heads (Fig. 4DII). In this case, the locus of deposition is displaced downslope and the streams dissect the pediments of the piedmont zone. In this study 81 alluvial/fluviol fan apex positions (telescopic fans sensu Bowman, 1978; Colombo, 2005) were identified and analysed in the piedmont zone of the Gastre Basin (Fig. 4A).

## 4. Results

### 4.1. Geomorphology, sedimentology and stratigraphy of the Gastre Basin during the Quaternary

Based on multiple geomorphological and sedimentological observations and on stratigraphic relationships, the Quaternary deposits of the Gastre Basin are interpreted to represent the superimposition of three large-scale geomorphological systems (i.e., GS-1, GS-2, GS-3; Fig. 5).

#### 4.1.1. GS-1 remnant sedimentary basin infill

System GS-1 consists primarily of epiclastic deposits of the Choiquepal Formation (Volkheimer, 1964). It rests unconformably above Neogene deposits (Bilmes et al., 2014), is interbedded with volcanic units of the GS-2 (see description below), and it is covered by a complex mosaic of geomorphologic units of the GS-3 (Fig. 5). We subdivided this alluvial-lacustrine system into two units: remnant fans/bajadas and shorelines.

In the piedmont area, the GS-1 is characterized by remnant fans/bajadas that are incised by the modern streams (Fig. 5). These remnant fans/bajadas are characterized by the development of mature soils that include Bt/Btk horizons (Soil Survey Staff, 1999) > 1.2 m thick (Fig. 6). The slopes of the remnant fans and bajadas range between 1° and 3°. At the surface, this unit presents ventifacts and varnished gravels. The deposits of these units are partially unsorted pebble- to cobble-grade, matrix-supported conglomerates with abundant fine- to coarse-grained sandy matrix (Fig. 6). Locally, the conglomerates show better sorting with some imbricated pebbles and a clast-supported texture. The coarse-grained nature and texture of these successions, together with their piedmont situation, suggest dominance of hyperconcentrated flow deposits (Blair and McPherson, 1994; Nichols, 2009), with minor occurrences of streamflow deposits.

In the more distal areas, closer to the basin floor, the GS-1 is defined by shorelines developed exclusively on top of the remnant fans and bajadas (Fig. 5). This unit displays the maximum heights of the basin floor zone at 864–867 m asl. The shoreline deposits consist of pebble-grade, moderately sorted, clast-supported conglomerates typical of gravelly lake-beach facies (Gilli et al., 2005; Fig. 5).

#### 4.1.2. GS-2 basaltic lava field

This geomorphological system is predominantly composed of volcanic and volcanoclastic rocks of the Crater and Moreniyeu formations (Ravazzoli and Sesana, 1977; Proserpio, 1978). It is developed on top and interbedded with the sedimentary deposits of the GS-1, and it is partially covered by the younger units of the GS-3 (Fig. 5). The basaltic lava field of the GS-2 is composed of two sub units: basaltic lava flows and spatter cones (sensu Sigurdsson et al., 2000; Fig. 7). Lava flows are mainly pahoehoe type (Sigurdsson et al., 2000) showing regional slopes



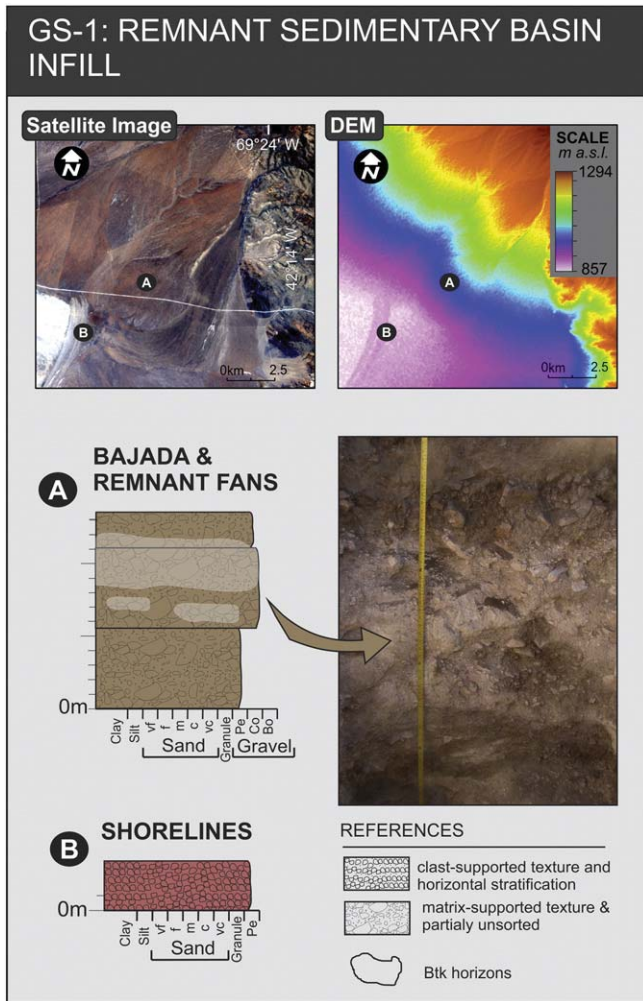


Fig. 6. Remnant sedimentary basin infill of the Gastre Basin (GS-1). Sedimentary logs, DEM data and field photographs of (A) bajada and remnant fan and (B) ancient shorelines.

of  $<3^\circ$ . The spatter cones (at least 25) were identified on the field and in satellite images and digital elevation models (Fig. 5). Field observations indicate that they are composed of spatter fragments and bombs with minor scoriaceous lapilli (Fig. 7). Their slopes range between  $18^\circ$  for the well-preserved cones and  $<1^\circ$  for the eroded ones. Several vents are aligned, indicating the existence of subsurface fractures that

determined the orientation of the feeder dykes (Massaferro et al., 2006; Bilmes et al., 2013). The association of lava flows and spatter cones points to the development of an  $\sim 600 \text{ km}^2$  basaltic lava field within the Gastre Basin (Fig. 5).

#### 4.1.3. GS-3 modern infill

The GS-3 is represented by the younger sedimentary infill of the Gastre Basin (Fig. 4). It includes all the deposits that are not grouped within a formal lithostratigraphic unit and that were informally described by previous authors as *depósitos modernos* (Ravazzoli and Sesana, 1977; Nullo, 1978; Proserpio, 1978; Volkheimer and Lage, 1981; Regairaz and Suivres, 1984; Bilmes, 2012). The deposits of the GS-3 are usually confined within remnants of the GS-1 and are linked to drainage systems that incise the older successions (i.e., GS-1 and GS-2). In some cases, the incisions associated to GS-3 caused topographic ridges up to 50 m high near the mountain front (Fig. 5). Deposits associated with GS-3 also appear to cover, at least partially, the volcanic rocks of the GS-2. Based on geomorphic characteristics, this geomorphological system was divided into four geomorphological units: small- to mid-scale distributive fluvial systems, shorelines, alluvial flats and playa lakes/salinars (Figs. 5, 8).

Small- to mid-scale distributive fluvial systems (radial size  $<30 \text{ km}$ ) are located in the piedmont (Bilmes and Veiga, 2016). Each distributive fluvial system (DFS; Hartley et al., 2010) has an ephemeral feeder channel that ends in alluvial flats and playa lakes/salinars units. The feeder channels are active only near the mountain front during wet seasons (usually winter or spring), whereas the distal part of these ephemeral streams could be inactive for several years. Only during some extraordinary winter storms (at least in the past 30 years, see methodology), small amounts of water are carried by the rivers from the mountain front to the distal playa lakes (Fig. 5). These DFS units have slopes between  $0.1^\circ$  and  $1^\circ$ , development of immature soil and lack of in situ ventifacts and varnished gravels at their tops. The DFS deposits consist of relatively well-sorted, pebble- to cobble-grade conglomerates with fine- to coarse-grained sandy matrix. Clast- and matrix-supported textures show planar cross-bedding, trough cross-bedding, horizontal stratification, and clast imbrication structures (Fig. 8). The overall geomorphological and sedimentological characteristics of these units suggest recurrence of streamflow processes (Smith, 1986; Blair and McPherson, 1994; Moscariello, 2005)

Closer to the basin floor, the geomorphological units of GS-3 are represented by the alluvial flats, beach ridges, and playa lakes/salinars (Fig. 5). The alluvial flat is the most extensive landform of the basin floor. It constitutes a nearly level vegetated surface (i.e., slopes  $<0.13^\circ$ ),  $<4 \text{ km}^2$  in extent, with small-scale topographic roughness. It consists predominately of massive sands associated with streamflow processes

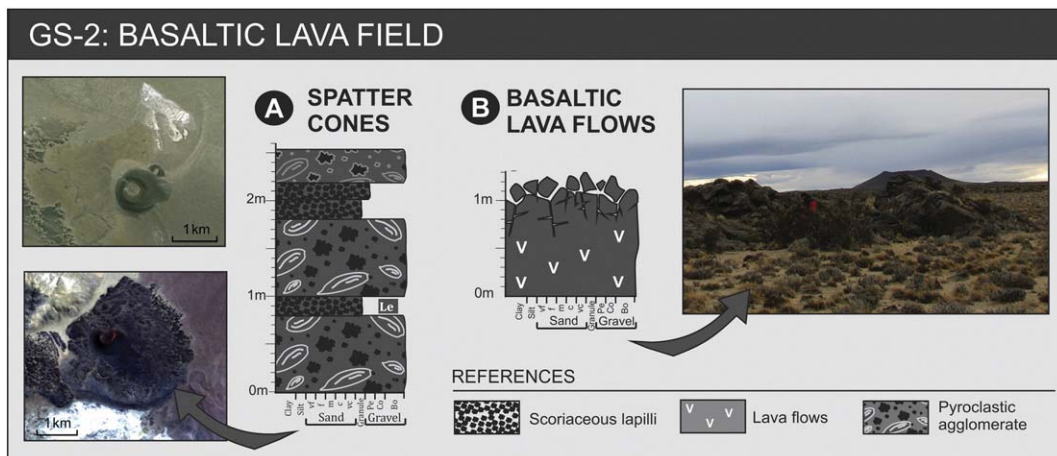
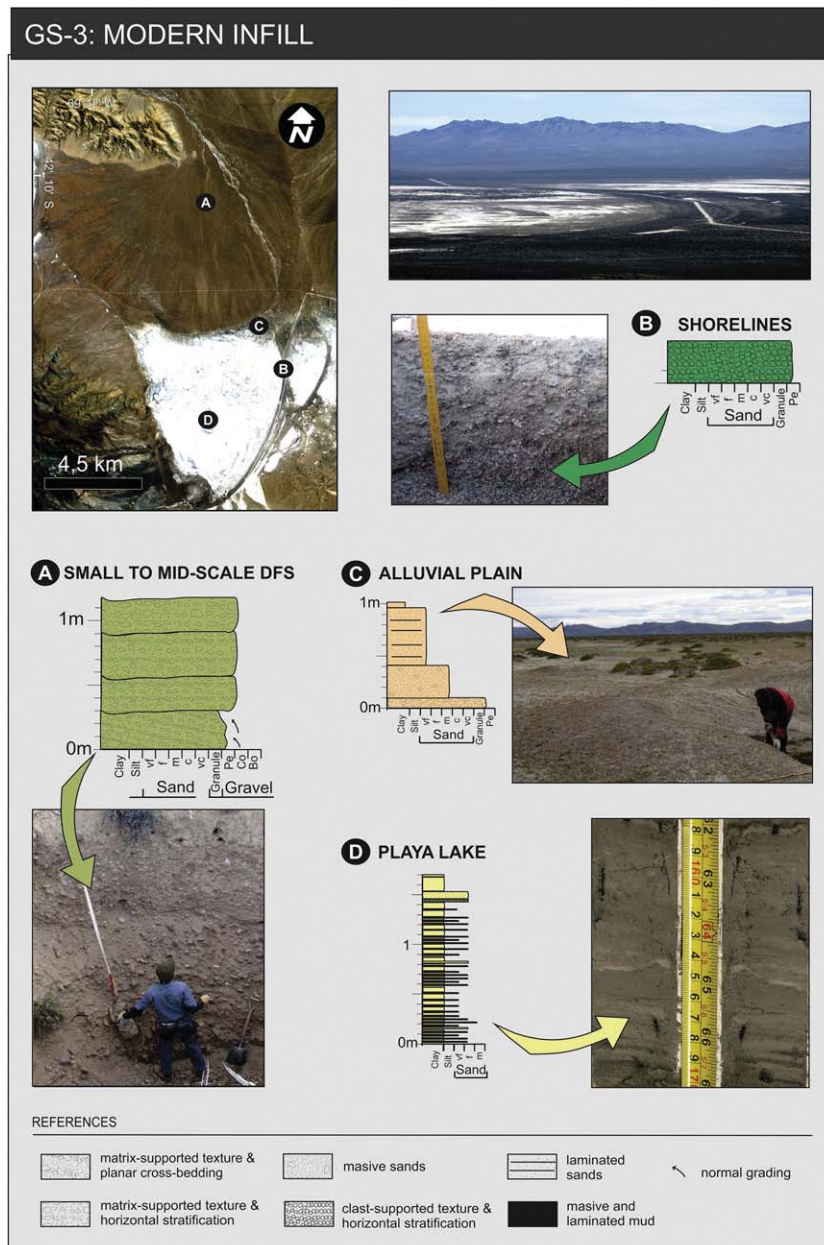


Fig. 7. Basaltic lava field of the Gastre Basin (GS-2). Sedimentary logs and field photographs of (A) spatter cones and (B) basaltic lava flows.



**Fig. 8.** Modern infill of the Gastre Basin (GS-3). Satellite image, sedimentary logs, and field photographs of (A) small- to mid-scale DFS, (B) shorelines, (C) alluvial plain, and (D) playa lakes.

(Fig. 8). To a lesser extent, laminated silts and muds, related to lacustrine and floodplain processes (lake plain deposits *sensu stricto* Peterson, 1981) are also present and partially cover the underlying streamflow deposits (Fig. 8).

Shorelines are characterized by several flat terraces located on the eastern side of the playa lakes/alluvial flats at different heights. In contrast to the shorelines of the GS-1, the shorelines of this geomorphological system developed even over GS-3 deposits (e.g., alluvial flat or DFS units) at heights below 861 m asl (Fig. 5). These units are made of gravelly lake-beach facies (Gilli et al., 2005) composed of pebble-grade, moderately sorted, clast-supported conglomerates (Fig. 8).

The fourth geomorphological unit of this system is the playa lakes/salinars. They are characterized by uniform flat areas (slope < 0.02°) where the water table generally is near the surface. They constitute shallow ephemeral lakes or salinas up to 60 km<sup>2</sup> in extent (e.g., Salina del Molle, Laguna Taquetrén; Figs. 2, 5). These units are composed of laminated muds and silts, interbedded with fine- to medium-grained sands (Fig. 7). Notably, ephemeral water bodies of the playa lakes

show very important fluctuations of volume, at least during the last 30 years. Maximum level of water of these water bodies occurs during austral winter months, when evapotranspiration is at its minimum.

#### 4.2. Age of the geomorphological-depositional systems

Most of the ages proposed in the literature for the Quaternary units of the Gastre Basin are relative ages based on stratigraphic relationships, which leads to discrepancy between authors. Only radiometric ages of basaltic lavas of the GS-2 gives some absolute constraint. Available ages in rocks of this system are comprised between  $1.9 \pm 0.4$  and  $0.23 \pm 0.1$  Ma (Mena et al., 2006; Pécskay et al., 2007; Haller et al., 2009), which constrain the GS-2 succession to the upper Gelasian to middle Pleistocene. The older deposits of the GS-1 (remnant sedimentary basin infill) are cover or interbedded with the basaltic lavas of the GS-2, constraining the age of GS-1 between Gelasian (or older) to the middle Pleistocene ( $\geq 1.9$  to  $\sim 0.23$ ). Finally, the stratigraphic relationship of the modern infill (GS-3) with the well-dated GS-2 and the presence of



immature soils in this system usually attributed to Holocene deposits (Peterson, 1981; Dunkerley and Brown, 1997) allow us to constrain the age of the GS-3 geomorphological system to the late middle Pleistocene–Holocene (<0.23 Ma to present).

4.3. Base-level evolution and paleohydrological reconstruction of the Gastre Basin

The relationship between the three geomorphological systems identified in the Gastre Basin suggests substantial base-level changes during its Quaternary evolution. Based on geomorphological, sedimentological, and stratigraphic evidence, three base-level stages have been determined (Fig. 9). In addition, for each of these stages, the water volume of the major lakes was calculated (Fig. 10).

The oldest and highest base-level of the Gastre Basin is indicated by the remnant fans/bajadas and shorelines of GS-1 (Figs. 5, 9A, B). Shorelines of this stage (stage 1) developed up to 867 m asl near the Taquetrén lake (+26 m above the current lake level) and up to 864 m asl near the Salina del Molle locality (+19 m above the current lake level; Figs. 5, 9, 10). Paleohydrological reconstruction of this stage indicates water volumes up to two orders of magnitude higher than the highest present-day values (i.e., 1347.9 km<sup>3</sup> for the Salina del Molle system and 1338.5 km<sup>3</sup> for the Laguna Taquetrén system; Fig. 10).

The small- to mid-scale DFSs and beach ridges of the GS-3 mark a second base-level stage of the Gastre Basin (stage 2). The fluvial network of this stage incised the remnant fan and bajadas of GS-1 by more than 50 m in the piedmont zone. At the basin floor, shorelines developed up to 861 m asl near the Laguna Taquetrén (i.e., +19 m above the current lake) and up to 856 m asl near the Salina del Molle (+14 m above the current lake; Figs. 5, 9A, C). Water-volume reconstructions for this stage are one order of magnitude higher than the highest present-day values (i.e., 368.2 km<sup>3</sup> for the Salina del Molle system and 675.1 km<sup>3</sup> for the Laguna Taquetrén system; Fig. 10).

Finally, the present-day base-level of the Gastre Basin is marked by the lowest topographic sector of the basin floor, the playa lake (Fig. 9D, E). Water bodies developed in this region (at least during the past

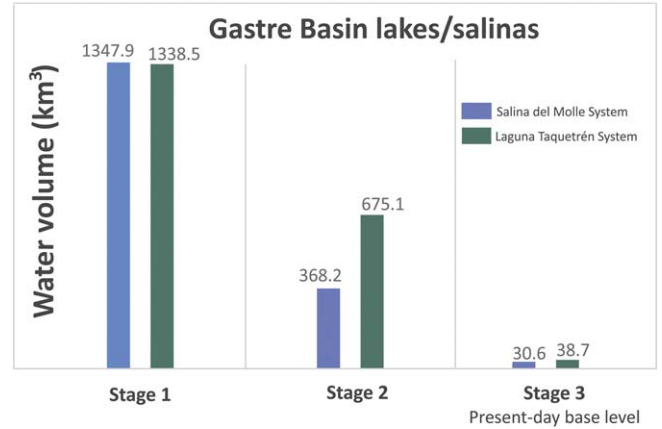


Fig. 10. Water volume reconstruction of major shallow lakes/salinas of the Gastre Basin.

30 years) mark the youngest base-level stage of the basin (stage 3). This stage includes periods of total desiccation of the shallow lakes (Fig. 9D) and high level periods when the ephemeral streams that came out of the mountain front were active and drained into the playa lakes (Fig. 9E). However, water-volume fluctuations during this stage are minimum in comparison with the water volumes recorded during previous stages (0 to 30.6 km<sup>3</sup> for the Salina del Molle system and 0 to 38.7 km<sup>3</sup> for the Laguna Taquetrén system; Fig. 10).

The three base-level stages recorded by geomorphic and sedimentary evidence in the study area imply at least two major base-level falls during the Quaternary history of the Gastre Basin. These base-level drops have magnitudes that do not match water level fluctuations observed in the past 30 years. Thus, we infer that a trigger mechanism not observed in recent times is needed to explain these base-level falls. Neotectonic activity and climate changes have long been described in the region (Gastre Basin and Carri Laufquen Basin; Volkheimer, 1965, 1972; Regairaz and Suivres, 1984; Galloway et al., 1988; Bradbury et al., 2001; Massafferro et al., 2006; Ariztegui et al., 2008; Cartwright et al.,

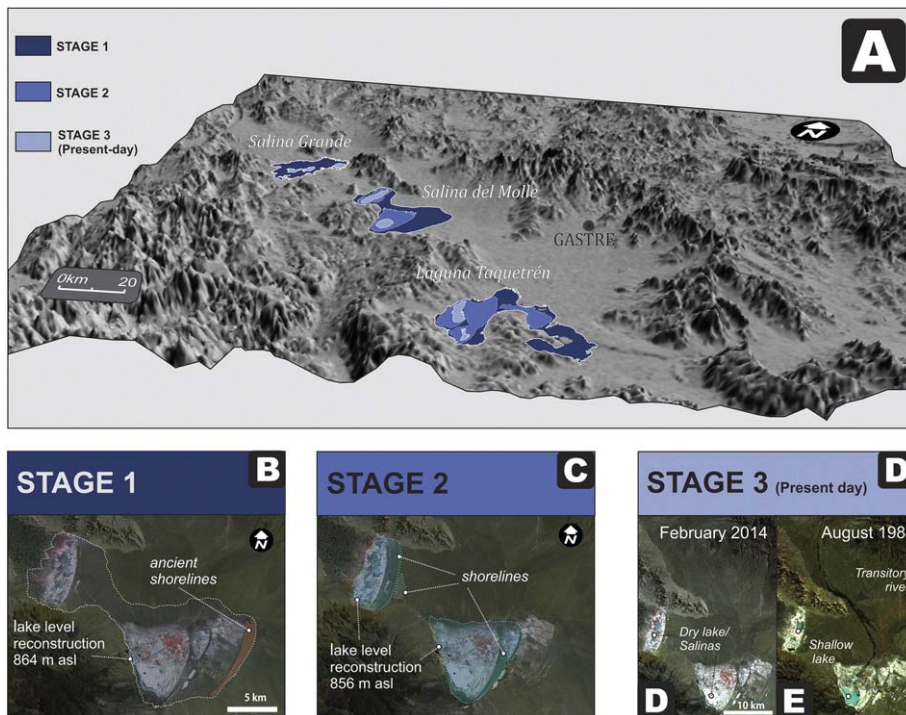


Fig. 9. Base-level stages in the Quaternary evolution of the Gastre Basin. (A) Three-dimensional model showing the three stages. (B) Satellite image of the Salina del Molle region with the reconstruction for stage 1. (C) Satellite image of the Salina del Molle region with the reconstruction of stage 2. (D) Satellite image of the Salina del Molle region with the reconstruction of stage 3. (E) Dry period; (F) wet period.



2011). Therefore, these seem to be the natural candidates for the mechanisms responsible of these base-level drops. In order to analyse if the tectonic activity was responsible for these changes in the Gastre Basin, a tectonic geomorphology analysis was carried out.

#### 4.4. Tectonic geomorphology analysis

Direct observation indicating the occurrence of Quaternary faults (e.g., piedmont fault scarps) were not found affecting neither the GS-1, GS-2, nor the GS-3 deposits. In addition, regional tectonic uplift can be ruled out as a trigger mechanism of base-level drops as it has been described as a long wave-length phenomenon that cannot affect base levels within a closed basin (Guillaume et al., 2009; Pedoja et al., 2011; Folguera et al., 2015). However, the asymmetry of the Gastre Basin (Fig. 2) and the presence of vent alignments in the lava field of GS-2 (Fig. 3) are potential evidence of Quaternary basin-scale crustal tectonics in the study area. To uncover possible patterns of neotectonic activity in the Gastre Basin, different morphometric analyses were carried out (see methodology) that included mountain front sinuosity indices ( $Smf$ ), valley width-height ratios ( $Vf$ ), and analysis of alluvial/fluvial fan apex position in the piedmont slope.

The overall morphometric data of the surrounding mountain front and piedmont zone of the Gastre Basin indicate moderate to high values of  $Smf$  (1.21–3.36; with 67% of the data showing higher values than 1.8) and high values of  $Vf$  (1.69–12.14; with 97.7% higher than 2.0; Fig. 11). In addition, alluvial/fluvial fans apex positions are observed up to 12 km away from the mountain front (Fig. 12). Notably, shifting fan heads and fan incision can result from tectonic and climate changes (Lecce, 1990; Gomez Villar, 1996; Burbank and Anderson, 2005), such that analysing a suite of fans bordering a basin and not isolating fan apex positions are important. On the other hand, increased variability among fans would imply that tectonics is an important control on fan segmentation (Burbank and Anderson, 2005). In the Gastre Basin the 81 alluvial/fluvial fan apex positions are observed far away from the mountain front;

thus, fan incision is dismissing neotectonic activity at least in the basin boundary.

The comparison of the Gastre data set with morphometric data of tectonically active areas in other parts of the world (Bull and McFadden, 1977; Rockwell et al., 1984; Silva et al., 2003; Bull, 2007; El Hamdouni et al., 2008; Fig. 13) precludes the identification of neotectonic activity in the Gastre Basin during the middle Pleistocene–Holocene (i.e., minimal tectonic activity during the Quaternary (sensu Bull, 2007) and inactive tectonic activity during the Quaternary (sensu Bull and McFadden, 1977; Rockwell et al., 1984; Silva et al., 2003; El Hamdouni et al., 2008).

#### 5. Factors triggering Quaternary base-level drops in the Gastre Basin: tectonic vs. climatic

The lack of neotectonic activity in the Gastre Basin during a period in which significant base-level drops are recorded implies that these major base-level reconfigurations were not triggered by tectonic activity. In addition, the absence of natural dams or outburst flood evidence dismisses lake outlet erosion in the Gastre Basin during the Quaternary. Paleohydraulic analyses for stages 1 and 2 indicate volumes of water in the systems before base-level drops that do not match with present-day climate of the region (Fig. 10). Therefore, climate conditions during stages 1 and 2 were considerably wetter, suggesting that a progressive shift toward drier climates could have been the trigger mechanism of the base-level falls.

The short to negligible transfer subsystems that feed the Gastre Basin (Fig. 2) imply that base-level oscillations observed within the basin represent geomorphic signals associated to climate changes that occurred in the sedimentation subsystem and in the source area (Castelltort and Van Den Driessche, 2003; Simpson and Castelltort, 2012).

Although paleoclimatic studies are absent in the Gastre Basin, in the neighbouring Carri Laufquen Basin (only 80 km north; Fig. 1), previous investigations correlate base-level reconfigurations during the

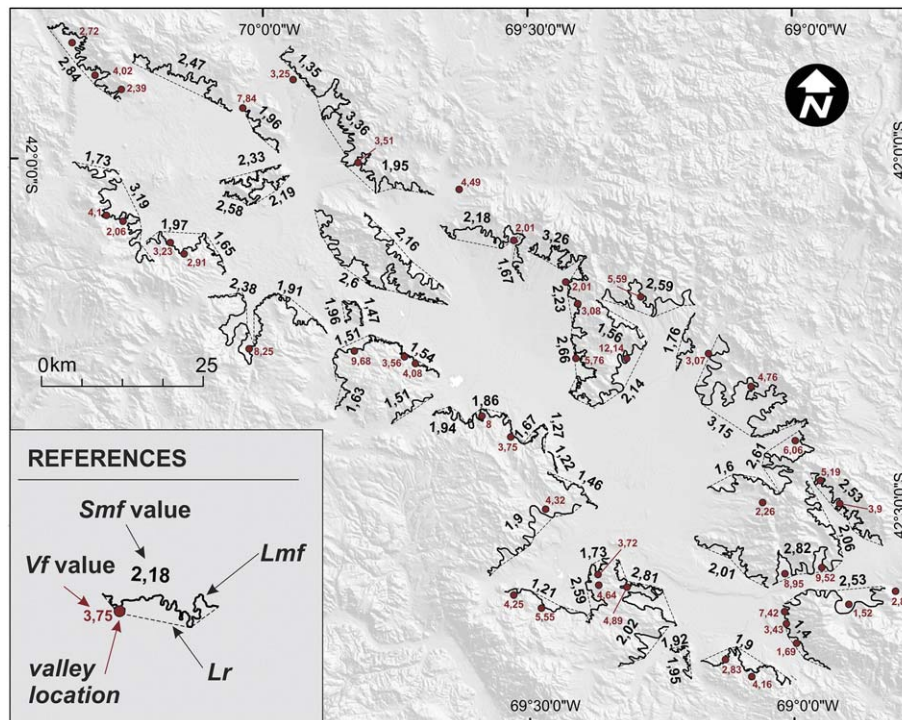
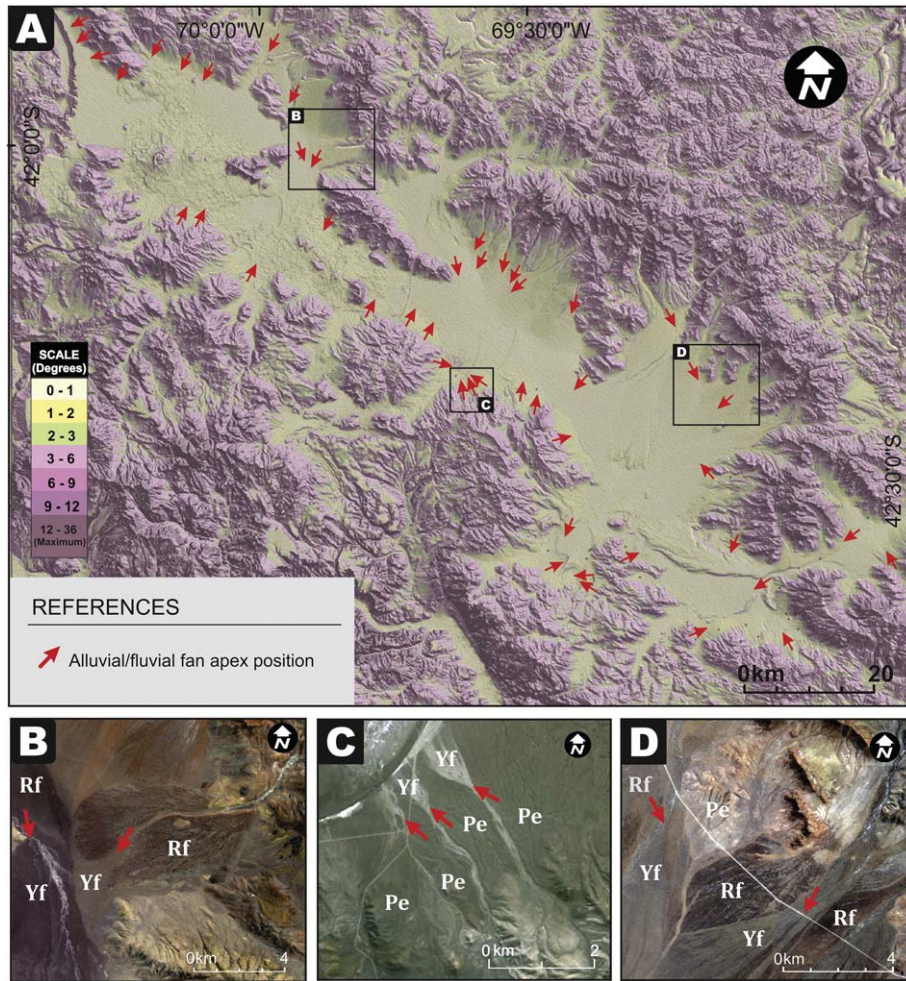
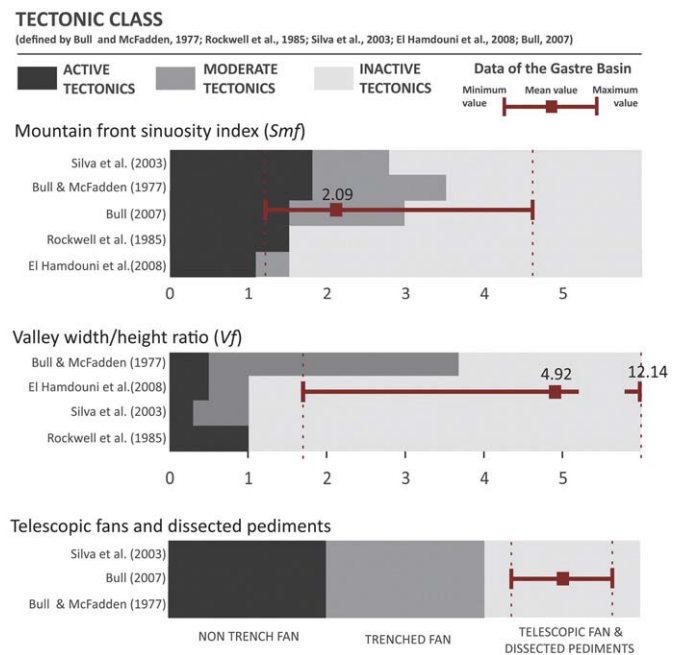


Fig. 11. Hillshade map of the Gastre Basin showing mountain front sinuosity index ( $Smf$ ) and valley width-height ratio ( $Vf$ ) locations and values.  $Lmf$ : length of the mountain piedmont junction;  $Lr$ : straight-line length of the associated range.



**Fig. 12.** (A) Slope map of the Gastre Basin with telescopic fans and dissected pediment locations (red arrows). (B), (C), and (D) Satellite images highlighting the relation between remnant fans, pediments, and younger fans (for location see the slope map). Rf: Remnant fan; Yf: Younger fan; Pe: Pediment.

Quaternary with climate change (Galloway et al., 1988; Ariztegui et al., 2001; Del Valle et al., 2007; Quade and Broecker, 2009; Cartwright et al., 2011). Furthermore, as in the Gastre Basin, higher paleoshorlines are visible in the Carri Laufquen Basin (e.g., in the Laguna Carri Laufquen Grande; Figs. 14A, B). The most prominent ones are two groups of shorelines that demonstrate high lake levels during the upper Pleistocene. The older has infinite ages >40 ka, whereas the younger was constrained to the Late Glacial Maximum (19 to 26 ka; Cartwright et al., 2011). The strong similarities between these neighbouring basins suggest a common evolution during the Quaternary, indicating that climate change could have been the main responsible mechanism of base-level falls also in the Gastre Basin. In addition, given their timing, shorelines of stages 1 and 2 of the Gastre Basin (Fig. 14C) could be equivalent to the two groups of shorelines identified in the Carri Laufquen Basin (Fig. 14B), suggesting that base level drops were rapid regional responses to climate change. This implies that the closed Gastre Basin can be viewed as a *reactive* landscape in the terminology of Allen (2008), that is, a landscape for which geomorphic system response was rapid with respect to the frequency of climatic perturbations. However, while it is suggested that climate change has been the main trigger mechanism of base-level falls in the Gastre Basin, further investigations are needed to understand the timing of lake-level fluctuations. Such an approach will allow us to discuss the extent to which a common *reactive* vs. *buffered* evolutionary model can be proposed. The latter is critical in any attempt to reconstruct the late Pleistocene-Holocene landscape response to climate change in the North Patagonian Foreland area.



**Fig. 13.** Comparison of the tectonic geomorphology of the Gastre Basin with tectonic classes defined in previous neotectonic studies.



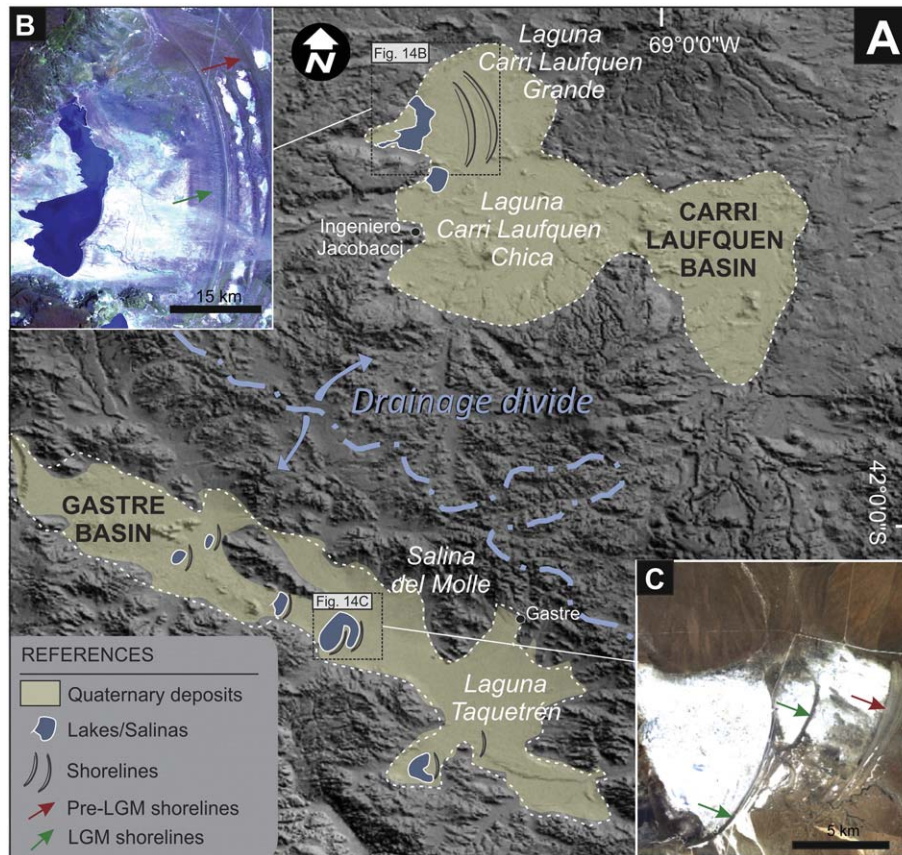


**Fig. 14.** Similarities between the Gastre and Carri Laufquen basins base-level drops. (A) Hillshade map of the study area with the location of the Gastre and Carri Laufquen basins. (B) Satellite image closeup of the Laguna Carri Laufquen Grande (Carri Laufquen Basin). (C) Satellite image closeup of the Salina del Molle (Gastre Basin).

## 6. Conclusions

Based on an extensive geomorphological survey, which includes new sedimentological, stratigraphic and tectonic geomorphology data of the Gastre Basin in the Patagonian Broken Foreland, base-level changes during upper-Pleistocene–Holocene have been described and interpreted. Three base-level stages were identified in a period during which no evidence of tectonic activity was found. These different stages document at least two major base-level drops in the upper Pleistocene history of the Gastre Basin. The available evidence indicates that these reconfigurations were rapid responses to climate perturbations and not to tectonics. The last dismiss any middle Pleistocene–Holocene tectonic fault activity for the Patagonian Broken Foreland in the Gastre Basin area. Finally, based on the scale as well as of the ages of the base level change recorded, we proposed that one of the base-level changes identified in the Gastre Basin could be correlated to climate variation after the last glacial maximum (LGM ~ 19 to 26 ka).

Supplementary data to this article can be found online at <http://dx.doi.org/10.1016/j.geomorph.2017.01.023>.

## Acknowledgements

The authors would like to thank the inhabitants of the study area for their support and hospitality. We are especially grateful to L. Lopez, M. Hernandez, and G. Álvarez for their assistance in the field and their friendship. The ALOS/JAXA images were provided for free by the CONAE. We also thank the editor Richard Marston and three anonymous reviewers for their helpful comments. This research was funded by the CONICET (PIP 5968, PIP 0632).

## References

- Allard, J.O., Giacosa, R., Paredes, J.M., 2011. Relaciones estratigráficas entre la Formación los Adobes (Cretácico inferior) y su sustrato Jurásico: implicancias en la evolución tectónica de la cuenca de Cañadón Asfalto, Chubut, Argentina. XVIII Congr. Geológico Argentino.
- Allen, P.A., 2008. From landscapes into geological history. *Nature* 451:274–276. <http://dx.doi.org/10.1038/nature06586>.
- Ariztegui, D., Anselmetti, F.S., Kelts, K., Seltzer, G., D'Agostino, A., 2001. Identifying paleoenvironmental change across South and North America using high-resolution seismic stratigraphy in lakes. In: Markgraf, V. (Ed.), *Interhemispheric Climate Linkages*. Academic Press, San Diego, pp. 227–240.
- Ariztegui, D., Anselmetti, F.S., Gilli, A., Waldmann, N., 2008. Late Pleistocene environmental change in Eastern Patagonia and Tierra del Fuego — a Limnogeological approach. In: Rabassa, J. (Ed.), *The Late Cenozoic of Patagonia and Tierra del Fuego*. Developments in Quaternary Sciences Series. Elsevier, pp. 241–253.
- Bilmes, A., 2012. Caracterización estratigráfica, sedimentológica y estructural del sistema de bajos neógenos de Gastre, provincias de Río Negro y de Chubut. Universidad Nacional de La Plata, La Plata (doi:ISBN 978-950-34-0840-7).
- Bilmes, A., Veiga, G.D., 2016. Linking mid-scale distributive fluvial systems to drainage basin area: geomorphological and sedimentological evidence from the endorheic Gastre Basin, Argentina. In: Ventra, D., Clarke, L.E. (Eds.), *Geology and Geomorphology of Alluvial and Fluvial Fans: Terrestrial and Planetary Perspectives*. Geological Society, London, Special Publications 440. <http://dx.doi.org/10.1144/SP440.4>.
- Bilmes, A., D'Elia, L., Franzese, J.R., Veiga, G.D., Hernández, M., 2013. Miocene block uplift and basin formation in the Patagonian foreland: the Gastre Basin, Argentina. *Tectonophysics* 601:98–111. <http://dx.doi.org/10.1016/j.tecto.2013.05.001>.
- Bilmes, A., D'Elia, L.D., Veiga, G.D., Franzese, J.R., 2014. Relleno intermontano en el Antepaís Fragmentado Patagónico: evolución neógena de la Cuenca de Gastre. *Rev. Asoc. Geol. Argent.* 71, 311–330.
- Blair, T.C., McPherson, J.G., 1994. Alluvial fans and their natural distinction from rivers based on morphology, hydraulic processes, sedimentary processes, and facies assemblages. *J. Sediment. Res.* 64, 450–489.
- Bowman, D., 1978. Determination of intersections points within a telescopic alluvial fan complex. *Earth Surf. Process.* 3, 265–276.
- Bradbury, J.P., Grosjean, M., Stine, S., Sylvestre, F., 2001. Full and Late Glacial records along the PEP1 transect: their role in developing interhemispheric paleoclimate interactions. In: Markgraf, V. (Ed.), *Inter-Hemispheric Climate Linkages*. Academic Press, San Diego, pp. 265–292.

- Bull, W.B., 1977. The alluvial fan environment. *Prog. Phys. Geogr.* 1, 222–270.
- Bull, W.B., 2007. *Tectonic Geomorphology of Mountains: A new Approach to Paleoseismology*. Blackwell, Malden.
- Bull, W.B., McFadden, L.D., 1977. Tectonic geomorphology north and south of the Garlock fault, California. In: Doehring, D.O. (Ed.), *Geomorphology in Arid Regions*. Publications in Geomorphology, State University of New York, Binghamton, pp. 115–138.
- Burbank, D.W., Anderson, R.S., 2005. *Tectonic Geomorphology*. Blackwell Science, Malden.
- Carroll, A.R., Bohacs, K.M., 1999. Stratigraphic classification of ancient lakes: balancing tectonic and climatic controls. *Geology* 27 (2):99–102. [http://dx.doi.org/10.1130/0091-7613\(1999\)027<0099:SCOALB>2.3.CO;2](http://dx.doi.org/10.1130/0091-7613(1999)027<0099:SCOALB>2.3.CO;2).
- Cartwright, A., Quade, J., Stine, S., Adams, K.D., Broecker, W., Cheng, H., 2011. Chronostratigraphy and lake-level changes of Laguna Cari-Laufquén, Río Negro, Argentina. *Quat. Res.* 76:430–440. <http://dx.doi.org/10.1016/j.yqres.2011.07.002>.
- Castellort, S., Van Den Driessche, J., 2003. How plausible are high-frequency sediment supply-driven cycles in the stratigraphic record? *Sediment. Geol.* 157:3–13. [http://dx.doi.org/10.1016/S0037-0738\(03\)00066-6](http://dx.doi.org/10.1016/S0037-0738(03)00066-6).
- CNEA, 1990. Estudio de Factibilidad y Anteproyecto de Ingeniería. Comisión Nacional de Energía Atómica, Buenos Aires.
- Coira, B.L., Nullo, F., Proserpio, C., Ramos, V.A., 1975. Tectónica de basamento en la región occidental del Macizo Norpatagónico (Prov. de Río Negro y Chubut) República Argentina. *Rev. Asoc. Geol. Argent.* 30, 361–383.
- Colombo, F., 2005. Quaternary telescopic-like alluvial fans, Andean Ranges, Argentina. *Geol. Soc. Lond. Spec. Publ.* 251:69–84. <http://dx.doi.org/10.1144/gsl.sp.2005.251.01.06>.
- Dalla Salda, L.H., Franzese, J., 1987. Las megafracturas del Macizo y la Cordillera norpatagónica y la génesis de las cuencas volcano-sedimentarias terciarias. *Rev. Geol. Chile* 31, 3–13.
- Del Valle, H.F., Tatur, A., Rinaldi, C.A., 2007. Cambios en lagos y circulación fluvial vinculados al calentamiento climático del Pleistoceno tardío-Holoceno temprano en Patagonia e Isla 25 de mayo, islas shetland del sur, Antártida. *Rev. Asoc. Geol. Argent.* 62, 618–626.
- Dorsaz, J.M., Gironás, J., Escarriaza, C., Rinaldo, A., 2013. The geomorphometry of endorheic drainage basins: implications for interpreting and modelling their evolution. *Earth Surf. Process. Landf.* 38:1881–1896. <http://dx.doi.org/10.1002/esp.3475>.
- Dunkerley, D.L., Brown, K.J., 1997. Desert soils. In: Thomas, D.S.G. (Ed.), *Arid Zone Geomorphology: Process, Form and Change in Drylands*. J. Wiley and Sons, New York, pp. 55–68.
- El Hamdouni, R., Irigaray, C., Fernández, T., Chacón, J., Keller, E.A., 2008. Assessment of relative active tectonics, southwest border of the Sierra Nevada (southern Spain). *Geomorphology* 96, 150–173.
- Figari, E.G., Courtade, S.F., Constantini, L.A., 1996. Stratigraphy and tectonics of Cañadon Asfalto Basin, Lows of Gastre and Gan Gan, North of Chubut Province, Argentina. *GeoResearch Forum*.
- Folguera, A., Ramos, V., 2011. Repeated eastward shifts of arc magmatism in the Southern Andes: a revision to the long-term pattern of Andean uplift and magmatism. *J. S. Am. Earth Sci.* 32, 1–16.
- Folguera, A., Gianni, G., Sagripanti, L., Rojas Vera, E., Novara, I., Colavitto, B., Alvarez, O., Orts, D., Tobal, J., Giménez, M., Introcaso, A., Ruiz, F., Martínez, P., Ramos, V.A., 2015. A review about the mechanisms associated with active deformation, regional uplift and subsidence in southern South America. *J. S. Am. Earth Sci.* 64:511–529. <http://dx.doi.org/10.1016/j.jsames.2015.07.007>.
- Galloway, R.W., Markgraf, V., Bradbury, J.P., 1988. Dating shorelines of lakes in Patagonia, Argentina. *J. S. Am. Earth Sci.* 1, 195–198.
- García-Castellanos, D., 2006. Long-term evolution of tectonic lakes: climatic controls on the development of internally drained basins. *Geol. Soc. Am. Spec. Pap.* 398: 283–294. [http://dx.doi.org/10.1130/2006.2398\(17\)](http://dx.doi.org/10.1130/2006.2398(17)).
- Gilli, A., Anselmetti, F.S., Ariztegui, D., Beres, M., McKenzie, J.A., Markgraf, V., 2005. Seismic stratigraphy, buried beach ridges and contourite drifts: the Late Quaternary history of the closed Lago Cardiel basin, Argentina (49°S). *Sedimentology* 52:1–23. <http://dx.doi.org/10.1111/j.1365-3091.2004.00677.x>.
- Gomez Villar, A., 1996. Abanicos Aluviales: Aportación teórica a sus aspectos más significativos. *Cuatern. Geomorf.* 10, 77–124.
- Guillaume, B., Martinod, J., Husson, L., Roddaz, M., Riquelme, R., 2009. Neogene uplift of central eastern Patagonia: dynamic response to active spreading ridge subduction? *Tectonics* 28, TC2009. <http://dx.doi.org/10.1029/2008tc002324>.
- Haller, M.J., Pécskay, Z., Németh, K., Gmélung, K., Massafiero, G.L., Meister, C.M., Nullo, F.E., 2009. Preliminary K-Ar geochronology of Neogene back arc volcanism in Northern Patagonia, Argentina. *IAVCEI-CVS-IAS-IMC Conf. Malargue, Argentina*, pp. 40–41.
- Hartley, A.J., Weissmann, G.S., Nichols, G., Warwick, G.L., 2010. Large distributive fluvial systems: characteristics, distribution, and controls on development. *J. Sediment. Res.* 80, 167–183.
- Howarth, J.D., Fitzsimons, S.J., Norris, R.J., Jacobsen, G.E., 2012. Lake sediments record cycles of sediment flux driven by large earthquakes on the Alpine fault, New Zealand. *Geology* 40:1091–1094. <http://dx.doi.org/10.1130/G33486.1>.
- Lecce, S.A., 1990. The alluvial fan problem. In: Rachocki, A., Church, M. (Eds.), *Alluvial Fans: A Field Approach*. John Wiley, Hoboken, pp. 3–24.
- Massafiero, G.L., Haller, M.J., D'Orazio, M., Alric, V.I., 2006. Sub-recent volcanism in Northern Patagonia: a tectonomagmatic approach. *J. Volcanol. Geotherm. Res.* 155, 227–243.
- Mena, M., Ré, G.H., Haller, M.J., Singer, S.E., Vilas, J.F., 2006. Paleomagnetism of the late Cenozoic basalts from northern Patagonia. *Earth Planets Space* 58, 1273–1281.
- Mon, R., Gutiérrez, A.A., 2009. The Mar Chiquita Lake: an indicator of intraplate deformation in the central plain of Argentina. *Geomorphology* 111, 111–122.
- Moscariello, A., 2005. Exploration potential of the mature Southern North Sea basin margins: some unconventional plays based on alluvial and fluvial fan sedimentation models. In: Dore, A.G., Vining, B.A. (Eds.), *Petroleum Geology: North-West Europe and Global Perspectives – Proceedings of the 6th Petroleum Geology Conference*. Geological Society of London, London, pp. 595–605.
- Nichols, G., 2009. *Sedimentology and Stratigraphy*. John Wiley and Sons, New York.
- Nullo, F.E., 1978. Descripción Geológica de la Hoja 41d, Lipetrén, Provincia de Río Negro. *Minist. Econ. Secr. Estado Minería, Boletín* 158, pp. 1–88.
- Pécskay, Z., Haller, M.J., Németh, K., 2007. Preliminary K/Ar geochronology of the Crater Basalt volcanic field (CBVF), northern Patagonia. *Rev. Asoc. Geol. Argent.* 62, 25–29.
- Pedoja, K., Regard, V., Husson, L., Martinod, J., Guillaume, B., Fucks, E., Iglesias, M., Weill, P., 2011. Uplift of quaternary shorelines in eastern Patagonia: Darwin revisited. *Geomorphology* 127:121–142. <http://dx.doi.org/10.1016/j.geomorph.2010.08.003>.
- Peterson, F.F., 1981. Landforms of the basin & range province defined for soil survey. *Technical Bulletin Nevada Agricultural Experimentation*. Nevada.
- Pochat, S., Van Den Driessche, J., Mouton, V., Guillocheau, F., 2005. Identification of Permian palaeowind direction from wave-dominated lacustrine sediments (Lodève Basin, France). *Sedimentology* 52:809–825. <http://dx.doi.org/10.1111/j.1365-3091.2005.00697.x>.
- Proserpio, C.A., 1978. Descripción Geológica de la Hoja 42d, Gastre, Provincia del Chubut (1:200000). *Minist. Econ. Secr. del Estado Minería, Boletín* 159, 76.
- Quade, J., Broecker, W.S., 2009. Dryland hydrology in a warmer world: lessons from the Last Glacial period. *Eur. Phys. J. Spec. Top.* 176:21–36. <http://dx.doi.org/10.1140/epjst/e2009-01146-y>.
- Rabassa, J., Clapperton, C.M., 1990. Quaternary glaciations of the southern Andes. *Quat. Sci. Rev.* 9:153–174. [http://dx.doi.org/10.1016/0277-3791\(90\)90016-4](http://dx.doi.org/10.1016/0277-3791(90)90016-4).
- Ravazzoli, I.A., Sesana, F.L., 1977. Descripción geológica de la hoja 41c-Río Chico. *Minist. Econ. Secr. Estado Minería, Boletín* 148, pp. 1–80.
- Regairaz, A.C., Suvires, G.M., 1984. Unidades Geomorfológicas en la depresión de Gastre, Provincia del Chubut. *Noveno Congr. Geológico Argentino*.
- Rockwell, T.K., Keller, E.A., Clark, M.N., Johnson, D.L., 1984. Chronology and rates of faulting of Ventura River terraces, California. *Geological Society of America Bulletin*: pp. 1466–1474. [http://dx.doi.org/10.1130/0016-7606\(1984\)95<1466:carofo>2.0.co;2](http://dx.doi.org/10.1130/0016-7606(1984)95<1466:carofo>2.0.co;2).
- Rodríguez, E., Morris, C.S., Belz, J.E., 2006. A global assessment of the SRTM performance. *Photogramm. Eng. Remote Sens.* 72:249–260. <http://dx.doi.org/10.14358/PERS.72.3.249>.
- Sigurdsson, H., Houghton, B.F., McNutt, S., Rymer, H., Stix, J., 2000. *Encyclopedia of Volcanoes*. Academic Press.
- Silva, P.G., Goy, J.L., Zazo, C., Bardají, T., 2003. Fault-generated mountain fronts in south-east Spain: geomorphologic assessment of tectonic and seismic activity. *Geomorphology* 50, 203–225.
- Simpson, G., 2014. Decoupling of foreland basin subsidence from topography linked to faulting and erosion. *Geology* 42:775–778. <http://dx.doi.org/10.1130/G35749.1>.
- Simpson, G., Castellort, S., 2012. Model shows that rivers transmit high-frequency climate cycles to the sedimentary record. *Geology* 40:1131–1134. <http://dx.doi.org/10.1130/G33451.1>.
- Smith, G.A., 1986. Coarse-grained nonmarine volcanoclastic sediment – terminology and depositional process. *Geol. Soc. Am. Bull.* 97, 1–10.
- Soil Survey Staff, 1999. *Soil Taxonomy. A basic system of soil classification for making and interpreting soil surveys*. Agricultural Handbook 436, second ed. Natural Resources Conservation Service, USDA, Washington.
- Volkheimer, W., 1964. Estratigrafía de la zona extra andina del departamento de Cushamen (Chubut), entre los paralelos de 42° y 42° 30' y los meridianos 70° y 71°. *Rev. Asoc. Geol. Argent.* 19, 85–107.
- Volkheimer, W., 1965. Bosquejo geológico del noroeste del Chubut extra andino (zona Gastre – Gualjaina). *Rev. Asoc. Geol. Argent.* 20, 326–350.
- Volkheimer, W., 1972. Sobre el origen de los bajos sin salida en la Patagonia Extraandina Septentrional. *Rev. Asoc. Geol. Argent.* 27, 410–412.
- Volkheimer, W., 1973. Observaciones geológicas en el área de Ingeniero Jacobacci y adyacencias (Provincia de río Negro). *Rev. Asoc. Geol. Argent.* 28, 13–36.
- Volkheimer, W., Lage, J., 1981. Descripción Geológica de la Hoja 42c, Cerro Mirador, Provincia de Chubut. *Ministerio de Economía, Secretaría de Estado de Minería, Boletín. Minist. Econ. Secr. Estado Minería, Boletín* 181, pp. 1–71.
- Wells, S.G., Bullard, T.F., Menges, C.M., Drake, P.G., Karas, P.A., Kelson, K.I., Ritter, J.B., Wesling, J.R., 1988. Regional variations in tectonic geomorphology along a segmented convergent plate boundary pacific coast of Costa Rica. *Geomorphology* 1, 239–265.
- Whittaker, A.C., 2012. How do landscapes record tectonics and climate? *Lithosphere* 4: 160–164. <http://dx.doi.org/10.1130/RF.L003.1>.
- Wünnemann, B., Yan, D., Ci, R., 2015. Morphodynamics and lake level variations at Paiku Co, southern Tibetan Plateau, China. *Geomorphology* 246:489–501. <http://dx.doi.org/10.1016/j.geomorph.2015.07.007>.
- Yrigoyen, M., 1969. Problemas estratigráficos del Terciario de Argentina. *Ameghiniana* 6, 349–356.